Glycoconj J (2013) 30:537–547
DOI 10.1007/s10719-012-9453-7

N-glycan analysis of human α1-antitrypsin produced in Chinese hamster ovary cells

Kyung Jin Lee · Sang Mee Lee · Jin Young Gil · Ohsuk Kwon · Jin Young Kim · Soon Jae Park · Hye-Shin Chung · Doo-Byoung Oh

Received: 1 August 2012 / Revised: 18 September 2012 / Accepted: 19 September 2012 / Published online: 12 October 2012

Abstract Human alpha-1-antitrypsin (α1AT) is a glycoprotein with protease inhibitor activity protecting tissues from degradation. Patients with inherited α1AT deficiency are treated with native α1AT (nAT) purified from human plasma. In the present study, recombinant α1AT (rAT) was produced in Chinese hamster ovary (CHO) cells and their glycosylation patterns, inhibitory activity and *in vivo* half-life were compared with those of nAT. A peptide mapping analysis employing a deglycosylation reaction confirmed full occupancy of all three glycosylation sites and the equivalency of rAT and nAT in terms of the protein level. *N*-glycan profiles revealed that rAT contained 10 glycan structures ranging from bi-antennary to tetra-antennary complex-type glycans while nAT displayed six peaks comprising majorly bi-antennary glycans and a small portion of tri-antennary glycans. In addition, most of the rAT glycans were shown to have only core α(1-6)-fucose without terminal fucosylation, whereas only minor portions of the nAT glycans contained core or Lewis X-type fucose. As expected, all sialylated glycans of rAT were found to have α(2-3)-linked sialic acids, which was in sharp contrast to those of nAT, which had mostly α(2-6)-linked sialic acids. However, the degree of sialylation of rAT was comparable to that of nAT, which was also supported by an isoelectric focusing gel analysis. Despite the differences in the glycosylation patterns, both α1ATs showed nearly equivalent inhibitory activity in enzyme assays and serum half-lives in a pharmacokinetic experiment. These results suggest that rAT produced in CHO cells would be a good alternative to nAT derived from human plasma.

Keywords Alpha1-antitrypsin · *N*-glycan · *In vivo* half-life · Sialic acid · Antennary structure · Chinese hamster ovary (CHO) cells

Electronic supplementary material The online version of this article (doi:10.1007/s10719-012-9453-7) contains supplementary material, which is available to authorized users.

Kyung Jin Lee and Sang Mee Lee contributed equally to this work.

K. J. Lee · J. Y. Gil · O. Kwon · D.-B. Oh (✉)
Korea Research Institute of Bioscience & Biotechnology (KRIBB),
125 Gwahak-ro, Yuseong-gu,
Daejeon 305-806, Korea
e-mail: dboh@kribb.re.kr

S. M. Lee · S. J. Park · H.-S. Chung
Alteogen Inc.,
Bioventure town,
Daejeon 305-812, Korea

J. Y. Gil · H.-S. Chung (✉)
Department of Biotechnology, Hannam University,
Daejeon 305-811, Korea
e-mail: hschung@hnu.kr

J. Y. Kim
Korea Basic Science Institute,
Ochang-eup,
Cheongwon-gun Chungbuk 363-883, Korea

K. J. Lee
Department of Biological Science, Wonkwang University,
Iksan 570-749, Korea

Introduction

Glycosylation is a key co- and/or post-translational modification, which adds a glycan to a polypeptide. More than 60 % of protein therapeutics is glycoproteins containing glycans, which play crucial roles in protein folding, therapeutic efficacy, *in vivo* half-lives and immunogenicity. Mammalian cells have become the predominant expression system for the production of therapeutic glycoproteins due to the structural similarity of their glycans with those of

humans. Among them, Chinese hamster ovary (CHO) cells have been most widely used since human tissue plasminogen activator produced in CHO cells was first approved in 1986 [1]. Currently, CHO cells have become the most important industrial cell line due to its many advantages. First, owing to their long and wide-ranging history of use, safety issues pertaining to their therapeutic application were clearly defined to meet the demands of regulatory authorities. Second, serum-free media and adaptation techniques were well developed, both of which minimize the use of animal-derived substances in the manufacturing processes. Third, cutting-edge technologies for the construction of recombinant cell lines and large-scale fed-batch suspension cultures have enabled the high-yield production of glycoproteins, with more than 10 g/liter of antibody production reported [2]. Fourth, compared to other mammalian cell lines such as murine myeloma SP2 and NS0, CHO cells have more 'human-like' glycosylation profiles. For example, minimal levels of the terminal galactose-α(1-3)-galactose (α-Gal) antigen, which can cause IgE-mediated anaphylaxis as reported in a murine myeloma cell-derived glycoprotein [3], were barely detected (less than ~0.2 %) in glycoproteins produced in CHO cells [4].

Alpha-1-antitrypsin (α1AT) is an inhibitor of serine proteases, especially neutrophil elastase, which degrades connective tissue in the lung. Therefore, if α1AT is not available, neutrophil elastase is free to break down elastin, resulting in respiratory complications such as emphysema. Its deficiency is a disorder inherited in an autosomal co-dominant fashion, which leads to the chronic destruction of lung parenchyma. Since the mid-1980, patients with α1AT deficiency have been treated with α1AT concentrates, which raised the levels of α1AT in the blood and tissues, thus slowing the progression of emphysema. Currently, all approved α1AT products are manufactured from large pools of human plasma through purification processes, which include pathogen reduction steps. As a result, they have considerable differences, and their activities range from 0.6 to 1 mg active α1AT per milligram of protein with less than 40 % plasma protein impurity levels [5]. Because this manufacturing process uses human plasma, there are risks of various infections, short supplies and batch-to-batch variations which originate from the different physicochemical properties of the starting donor pools. A good alternative manufacturing method for solving these problems would be the production of recombinant protein. Recombinant expressions of α1AT have been reported in various hosts, including *Escherichia coli* [6], *Saccharomyces diastaticus* [7], and *Aspergillus niger* [8]. These proteins, produced in bacteria, yeast and fungi, cannot be used for therapeutic purposes because either there is no glycosylation or their glycosylation patterns are significantly different from those of humans. Recently, Blanchard *et al.* expressed α1AT in a novel human neuronal cell line without the problem of different glycosylation patterns [9]. Diverse glycan structures ranging from bi- to tetra-antenna structures were observed, and most of them were found to be core α(1-6)-fucosylated together with some portion of the Lewis X epitope. Unfortunately, high portions of neutral glycans (11 %) and glycans lacking the terminal capping of sialic acids (41 %) were observed [9], which would lead to a reduced *in vivo* half-life.

In the present study, we produced recombinant α1AT (rAT) in a CHO cell, which is a widely used and validated cell line. Its sialic acid content, glycosylation pattern, biological activity and *in vivo* half-life were analyzed for a comparison with those of native α1AT (nAT) purified from human serum.

Materials and methods

Materials

Peptide-*N*-glycosidase F (PNGase F), graphitized carbon column (Carbograph) and nAT were purchased from New England Biolabs (Ipswich, MA, USA), Alltech (Lexington, MA, USA), and Calbiochem (Now Merck, Darmstadt, Germany), respectively. All of the exoglycosidases were bought from Prozyme (San Leandro, CA, USA) except for almond meal fucosidase (QA-Bio, Palm Desert, CA, USA). Biotinylated *Maackia amurensis* lectin (MAA) and *Sambucus nigra* (SNA) were obtained from Ey Laboratories (San Mateo, CA, USA) and Vector Laboratories (Burlingame, CA, USA), respectively. *Aspergillus oryzae* lectin (AOL) purchased from Tokyo Chemical Industry (Tokyo, Japan) was biotinylated using a biotin protein labeling kit from Roche (Manheim, Germany). Trypsin and ^{18}O-water ($H_2{}^{18}O$) were acquired from Promega (Madison, WI, USA), and Cambridge Isotope Laboratories (Andover, MA, USA), respectively. Solvents including HPLC-grade water and acetonitrile were purchased from Burdick and Jackson (Muskegon, MI, USA). Native α1AT purified from human plasma was purchased from Calbiochem. The other chemicals were obtained from Sigma-Aldrich (St. Louis, MO, USA) unless stated otherwise.

Recombinant expression in Chinese hamster ovary cells

The gene-encoding α1AT protein was amplified from the human cDNA clone hMU001448 (21C Frontier Human Gene Bank, KRIBB, Daejeon, Korea) by a polymerase chain reaction (PCR) using forward (5′-CCC TCC TCG AGA ATG CCG TCT TCT GTC TCG) and reverse (5′-GGG CCC GCG GCC GCA GTT ATT TTT GGG TGG G) primers. The PCR product was subcloned into the Xho I and Not I sites of the pAV1 vector, resulting in the expression vector pAV1-rAT. Chinese hamster ovary (CHO)-K1 cells

were grown in Isocove's Modified Dulbecco's Medium supplemented with 10 % FBS at 37°C in a 5 % CO_2 humidified incubator. Cells were grown to 80–90 % confluence and transfected with pAV1-rAT using polyethyleneimine (Polyscience Inc., Warrington, PA, USA) according to the manufacturer's instructions.

Purification of rAT

The culture supernatant was diluted with an equal volume of buffer A (20 mM sodium phosphate, pH 8.0) and was applied to a Q-Sepharose FF column (GE Healthcare, Piscataway, NJ, USA) equilibrated with the buffer A. The column was washed with equilibration buffer and eluted with a linear gradient (70–400 mM) of sodium chloride in the buffer A. Fractions containing rAT protein were pooled and directly loaded onto a AT select column (GE Healthcare) equilibrated with buffer B (50 mM Tris–HCl, pH 7.5, 150 mM NaCl). The rAT was eluted with a 0–0.5 M gradient of a $MgCl_2$ solution. The pooled fractions were concentrated using Vivaspin 20 (GE Healthcare) and dialyzed against phosphate-buffered saline (PBS).

Gel electrophoresis and lectin blot

The nAT and rAT sizes were compared by sodium dodecyl sulfate-polyacrylamide gel electrophoresis (SDS-PAGE) after partial and full deglycosylation using varying amounts (0, 5, 12.5 and 25 NEB unit) of PNGase F for an occupancy analysis. First, five μg of glycoprotein samples were denatured in 10 μl of a denaturing buffer (0.5 % SDS, 40 mM DTT) by boiling for 5 min. After cooling to room temperature, the denatured glycoprotein solutions were incubated in 20 μl of G7 reaction buffer (50 mM sodium phosphate, pH 7.5) containing 1 % NP-40 with PNGase F for 5 min. After boiling for 5 min to stop the deglycosylation reaction, the resulting solutions were applied to SDS-PAGE. For a determination of the charged status, isoelectric focusing (IEF) was carried out in 1.0 mm Novax® IEF gels in the pH range of 3 to 7 (Invitrogen, Carlsbad, CA, USA) according to the manufacturer's instructions. Lectin blot analyses were performed as described previously [10]. Briefly, 2 μg of nAT and rAT were subjected 8 % SDS-PAGE and then transferred to a PVDF membrane. After a blocking step using 3 % bovine serum albumin, the membranes were incubated with biotinylated-MAA (1 μg/ml), -SNA (0.8 μg/ml) and –AOL (0.3 μg/ml). As a secondary reagent, horseradish peroxidase-conjugated streptavidin (Millipore, Billerica, MA, USA) was used. After extensive washing steps, the resulting membrane was visualized using ECL Western blot detection reagents (GE Healthcare).

Analysis of tryptic peptides and glycosylation sites

The conversion of glycosylated Asn into ^{18}O-tagged Asp by PNGase F was carried out as previously described [11] with slight modifications. Briefly, 50 μg of dried protein samples were dissolved in 80 μl of 50 mM of an ammonium bicarbonate buffer containing 0.1 % of RapiGest (Waters, Milford, MA) and 10 mM of DTT. The solution was incubated for 30 min at 60 °C with a subsequent addition of 9 μl of 150 mM iodoacetamide and incubation again in the dark for 30 min. Then, 1 μg of trypsin was added and this was incubated overnight at 37 °C. Next, after the addition of Pefabloc SC (Roche) and further incubation for 2 h, the mixture was dried.

The dried peptide samples were dissolved in mobile phase A for Nano-LC/ESI-MS/MS. Peptides were identified using MS/MS with a nano-LC-MS system consisting of a Nano Acquity UPLC system (Waters, Milford, MA, USA) and a LTQ-FT mass spectrometer (ThermoFinnigan, USA) equipped with a nano-electrospray source. An autosampler was used to load 4 μL aliquots of the peptide solutions onto a C_{18} trap-column (5 μm, 300 μm×5 mm; Waters). The peptides were desalted and concentrated on the column at a flow rate of 5 μL/min. The trapped peptides were then back-flushed and separated on a 100-mm home-made microcapillary column consisting of C_{18} (Aqua; particle size 3 μm) packed into 75-μm silica tubing with an orifice i.d. of about 6 μm. The mobile phases, A and B, were composed of 0 and 100 % acetonitrile, respectively, and each contained 0.1 % formic acid. The LC gradient began with 5 % B for 5 min and was ramped to 15 % B over 5 min, to 50 % B over 35 min, to 95 % B over 5 min, and remained at 95 % B over 5 min and 5 % B for another 5 min. The column was re-equilibrated with 5 % B for 15 min before the next run. The voltage applied to produce an electrospray was 2.2 kV. In each duty circle of mass analysis, one high-mass resolution (100,000) MS spectrum was acquired using the FT-ICR analyzer, followed by five data-dependent MS/MS scans using a linear ion trap analyzer. For the MS/MS analysis, normalized collision energy (35 %) was used throughout the collision-induced dissociation (CID) phase. All MS/MS spectral data were manually analyzed for peptide identification.

High-performance liquid chromatography (HPLC) analysis of sialic acids

The sialic acids were released from the α1AT samples by mild acid hydrolysis in 0.1 M HCl solution at 80 °C for 1 h. After cooling to room temperature, the acid hydrolysates were labeled using a fluorescence labeling kit using 1,2-diamino-4,5-methylenedioxybenzene (DMB) (TaKaRa) according to the manufacturer's instructions. After centrifugation at 10,000 rpm for 5 min, the aliquots of labeled sialic acids were analyzed on a Zorbox ODS C18 column (5 μm, 4.6 mm×

150 mm, Agilent, CA, USA) using a Waters Alliance system equipped with a Waters 2475 fluorescence detector. Elution was performed using a mixture of acetonitrile (9 %), methanol (7 %), and water (84 %) at a flow rate of 0.9 mL/min. Fluorescence was monitored with excitation and emission wavelengths of 373 nm and 448 nm, respectively. The concentrations of sialic acids in the samples were determined by using known amounts of sialic acids as a standard.

Release and purification of *N*-glycan

For the release of glycans, 50 μg of nAT or rAT was deglycosylated with 500 NEB unit of PNGase F at 37 °C overnight according to the manufacturer's instructions. The released *N*-glycans were purified by solid-phase extraction using graphitized carbon resin based on a previously described method [12]. Briefly, the solutions containing glycans were absorbed onto a pre-activated graphitized carbon column. After several washing steps using distilled water, the glycans were eluted by 25 % (v/v) acetonitrile in water containing 0.075 % trifluoroacetic acid. Solutions of purified glycans were dried for further modification and/or analysis.

Solid-phase permethylation and mass spectrometry

Dried glycans were re-dissolved in a mixture of 90 μl dimethyl sulfoxide (DMSO), 2.7 μl water, and 35 μl iodomethane and were then permethylated according to the solid-phase method as previously described [13, 14]. The resulting permethylated glycans were resuspended in 4 μl of a 50 % methanol solution. They were then mixed in equal volumes with 10 mg/ml 2,5-dihydroxybenzoic acid prepared in 1 mM of a sodium acetate solution. The resulting mixture was applied onto a MALDI MSP96 polished steel chip (Bruker Daltonik, GmbH, Bremen, Germany) and dried in air for matrix-assisted laser-desorption-ionization time-of-flight (MALDI-TOF) mass spectrometry. Permethylated glycans were analyzed in the reflector positive ion mode using a Microflex (Bruker Daltonik) while 2-aminobenzoic acid (AA)-labeled glycans were analyzed in the linear negative ion mode. All mass spectra were acquired at an acceleration voltage of 20 kV with the method recommended by manufacturer [13].

HPLC analysis of AA labeled glycans

For detection in the HPLC analysis, purified glycans were labeled AA as previously described [15] with slight modifications. Briefly, the labeling reagent was freshly prepared by dissolving 6 mg of AA in 100 μl 30 % (v/v) acetic acid in a dimethylsulphoxide solution containing 1 M of sodium cyanoborohydride. Then, each dried glycan sample was dissolved in 5 μl of a labeling reagent and incubated in a tightly capped tube at 37 °C overnight. After cooling, the mixture was diluted with 1 ml of 96 % (v/v) acetonitrile in water, and excess labeling reagent was removed using a cyano-SPE cartridge (Agilent Technologies, Santa Clara, CA) following the manufacturer's instructions. Purified AA-labeled glycans were separated on a TSK amide-80 (5 μm, 4.6 mm×250 mm) column (Tosoh Bioscience, Prussia, PA, USA) using the previously described HPLC systems with a fluorescence detector (360 nm excitation and 425 nm emission). Separations were achieved at a flow rate of 1.0 ml/min using a mixture of solvent A (100 % acetonitrile) and solvent B (50 mM ammonium formate, pH 4.4). After the column was equilibrated with 30 % solvent B, the sample was injected and then eluted by a linear gradient to 45 % solvent B for 80 min. The eluted fractions corresponding to the glycan peaks were collected and their masses were identified by mass spectrometry as described above.

Exoglycosidase digestions

Intact or AA-labeled glycans were digested in 20 mM ammonium acetate pH 5.0 at 37 °C for 16 h using exoglycosidase. The following units of exo-glycosidase were used in a 20 μl reaction: 10 mU *Streptococcus pneumonia* α(2-3)-sialidase (Sialidase S™, SPS), 70 mU *Salmonella typhimurium* α(2-3/6/8/9)-sialidase (Sialidase T™, STS), 1 mU *Streptococcus pneumonia* β(1-4)-galactosidase (SPG), 5 mU bovine testis β(1-3/4) galactosidase (BTG), 5 mU Jack bean β(1-2/3/4/6)-*N*-acetyl hexosaminidase (JBH), 5 mU bovine kidney α(1-2/3/4/6)-fucosidase (BKF), and 20 mU almond meal α(1-3/4)-fucosidase (AMF). After incubation, the reaction was stopped by boiling for 5 min and the sample was dried for further analysis.

Enzyme assay

The inhibitory activities of α1AT proteins were measured against human neutrophil elastase (HNE) and porcine pancreatic elastase (PPE) (Calbiochem) as previously described [16] with slight modifications. Briefly, inhibition assays were performed in an assay buffer (20 mM Tris–HCl, pH 8.0, 0.01 % Tween 80 and 5 mM $CaCl_2$) using *N*-MeO-succinyl-Ala-Ala-Pro-Val-*p*-nitroanilide and *N*-succinyl-$(Ala)_3$-*p*-nitroanilide as HNE and PPE substrates, respectively. Prior to substrate addition, 10 nM of enzyme was incubated with an equimolar concentration of rAT or nAT (elastase : α1AT = 1:1) for 30 min at room temperature. The reaction was then started by the addition of 1 mM substrate and the resulting product formation was monitored by the absorbance at 405 nm.

Pharmacokinetic assay

Single-dose pharmacokinetic studies were conducted using male Sprague–Dawley rats (9 weeks old). α1AT proteins

(10 nmol/kg dose) were intravenously administered to 3 rats via the tail vein. Blood samples were collected at the indicated time points after administration. Concentrations of antitrypsin in serum were determined by a sandwich enzyme-linked immunosorbent assay using two monoclonal anti-α1AT antibodies purchased from Medix Biochemica (Kauniainen, Finland). The detection antibody was biotinylated and recognized by the streptavidin-horseradish peroxidase conjugate.

Results

Size and charge comparison between rAT and nAT

The size of rAT purified from the culture supernatant of CHO cells was compared with that of nAT according to the electrophoretic mobilities in 10 % reducing SDS-PAGE (Fig. 1a). Both displayed nearly identical mobility levels in either glycosylated (~55 kDa) or deglycosylated form (~45 kDa) by PNGase F digestion. When digested partially with PNGase F, mobility patterns with zero to three *N*-glycosylation sites were detected in both proteins, indicating that the glycosylation sites of rAT produced in CHO cells are also fully occupied (Fig. 1c). An IEF gel image of the nAT used in this study exhibits multiple isoforms found in serum α1AT derived from healthy people (Fig. 1b) [17].

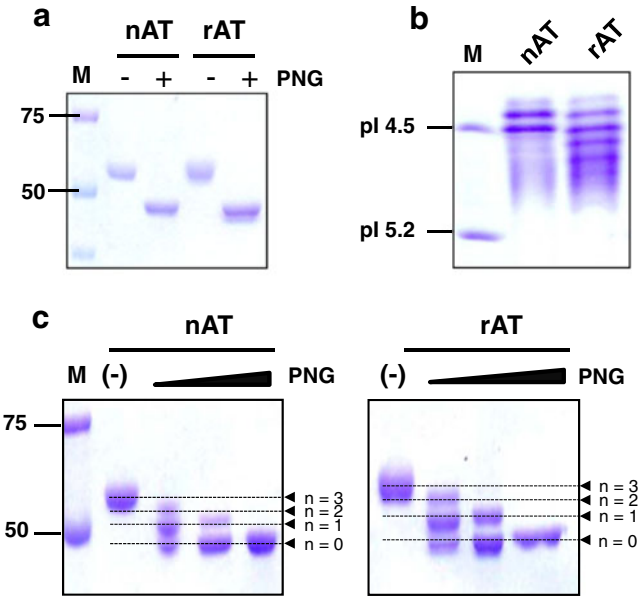

Fig. 1 Comparison of sizes and charges of nAT and rAT. **a** 10 % SDS-PAGE gel of nAT and rAT with/without PNGase F digestion (PNG). **b** Isoelectric patterns of nAT and rAT by IEF gel (pH 3–7). **c** Analysis of glycosylation occupancy by partial deglycosylation with PNGase F. Denatured α1ATs were digested in a short time (5 min) with increasing amounts (0, 5, 12.5 and 25 NEB unit) of PNGase F. 'n' indicates the number of *N*-glycosylation sites

The IEF pattern of rAT also showed the existence of similar multiple isoforms with the parallel regions, which may reflect equivalency with those of nAT in terms of the degree of sialylation. Notably, the intensities of multiple isoforms of rAT were more evenly distributed in contrast to the dominant intensities of the major two bands of nAT.

The equivalency of nAT and rAT in terms of the protein level was also confirmed by a comparison of the tryptic peptide mapping profiles after glycan removal by PNGase F (Supplementary Fig. S1). Furthermore, their full occupancies were cross-checked by the PNGase F digestion of the glycopeptides in ^{18}O water. When PNGase F cleaves the amide bond between the asparagine of peptide and the innermost GlcNAc, asparagine is converted to aspartic acid, resulting in an increase of 1 Da. To discriminate this reaction from naturally occurring deamidation, PNGase F digestion was carried out in ^{18}O water, leading to a mass increase of 3 Da. We performed this PNGase F-mediated tagging of the ^{18}O isotope after the addition of a trypsin inhibitor in order to minimize the C-terminal ^{18}O incorporation catalyzed by residual trypsin activity [11]. Three peptide sequences with a mass increase of 3 Da were found in a liquid chromatography/tandem mass spectrometry (LC/MS/MS) analysis (Supplementary Fig. S2-4). The masses of these peptides were in good agreement with those predicted from the previously known glycosylation sites (Asn46, Asn83 and Asn247). In this experiment, the peptide sequences expected by unoccupied glycosylation were not observed, indicating the full occupancy of rAT glycosylation.

Different *N*-glycan profiles of rAT and nAT

The *N*-glycans released from α1AT proteins by PNGase F digestion were either labeled with AA for HPLC analysis or modified by solid-phase permethylation for mass analysis using MALDI-TOF. Normal-phase HPLC was carried out using a TSK Amide-80 column, from which the labeled glycans were eluted mainly based on size, with larger *N*-glycans eluted later regardless of their charge (Fig. 2). There were 10 peaks detected in the HPLC profile of rAT, while six peaks were found in nAT. These 10 peaks could be matched well with the 10 peaks detected in the MALDI-TOF profile of the rAT glycans when considering the order of size and the corresponding relative intensity levels (Fig. 3). All of the peaks in HPLC were further characterized by mass analyses of the eluted fractions using MALDI-TOF (data not shown) and sequential exoglycosidase digestions (Fig. 2). The relative amount of each identified peak was calculated by integrating the peak area. These are represented as percentages in Table 1.

A chromatogram of the nAT glycans displayed one dominant major peak and five minor peaks (Fig. 2a), as previously reported [5]. The first four peaks had bi-antennary

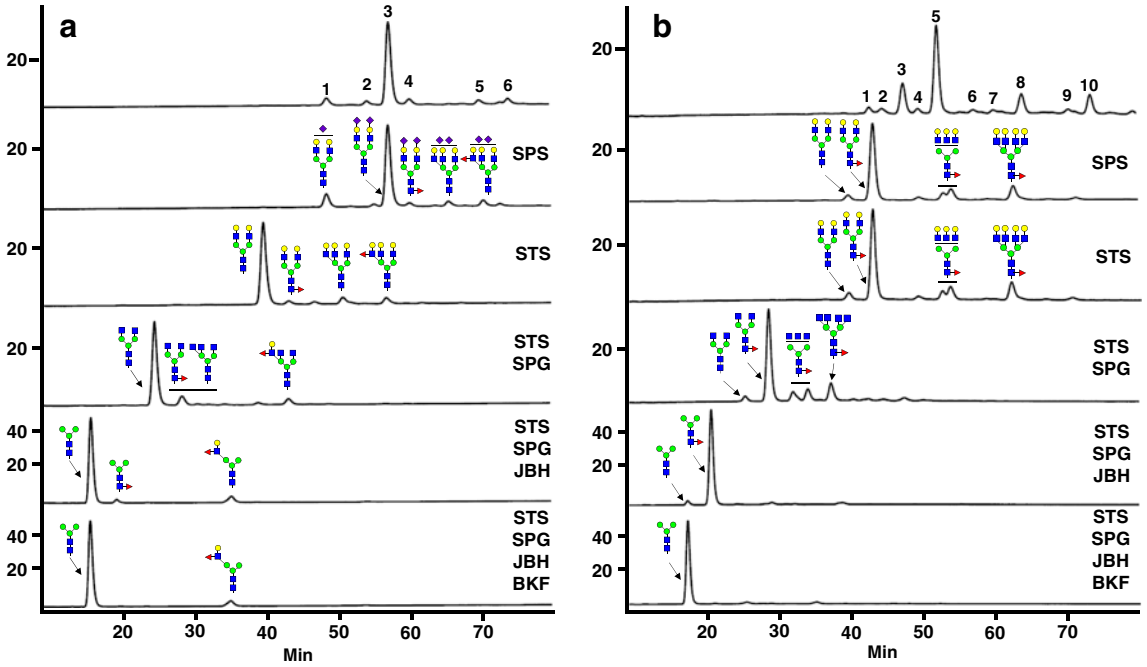

Fig. 2 Normal-phase HPLC profile of AA-labeled glycans. Glycans obtained from nAT (**a**) and rAT (**b**) were separated using a TSK Amide-80 column mainly based on their sizes. The top profiles display undigested glycans followed by a series of exoglycosidase digestions in the lower panels. The exoglycosidases were *Streptococcus pneumonia* sialidase (SPS), *Salmonella typhimurium* sialidase (STS), *Streptococcus pneumonia* galactosidase (SPG), Jack bean *N*-acetyl hexosaminidase (JBH), and bovine kidney fucosidase (BKF). The glycan structures, proportions, compositions and masses of the peaks indicated by the number in the top panels are summarized in Table 1. Symbols used for the representation of the glycan structures are those suggested by the Consortium for Functional Glycomics (http://www.functionalglycomics.org/). *Blue square*: GlcNAc, *green circle*: mannose, *yellow circle*: galactose, *purple diamond*: sialic acid, *red triangle*: fucose

glycan structures (91.6 %) constituting a large majority, in contrast with the tri-antennary structures of the last two minor peaks (8.4 %). Only small portions (10.2 %) of all glycan pools were shown to contain fucose residue. On the other hand, the glycans released from rAT were shown to have even tetra-antennary glycan structures (13.4 %) as well as bi- (63.4 %) and tri-antennary (13.4 %) structures. Also, most of the glycans (94.5 %) contained a fucose residue. The most dominant peak was fully sialylated bi-antennary glycan containing a fucose (A2G2FS2, peak 5 in Table 1), and this was followed by three major peaks of the mono-sialylated bi-antennary glycan (A2G2FS, peak 3) and fully sialylated tri- (A3G3FS3, peak 8) and tetra-antennary glycans (A4G4FS4, peak 10).

Comparison of sialic acid contents

Most of the glycans of rAT were found to be capped with terminal sialic acids in the HPLC profile, while neutral glycans accounted for only 3.3 %. The average number of sialic acids attached to one protein molecule could be calculated from the percentages of *N*-glycans with different degrees of sialylation [18]. The equation applied is as follows:

$$\left(\frac{1\,\mathrm{x}\,\%\mathrm{A}_{1\mathrm{SA}} + 2\,\mathrm{x}\,\%\mathrm{A}_{2\mathrm{SA}} + 3\,\mathrm{x}\,\%\mathrm{A}_{3\mathrm{SA}} + 4\,\mathrm{x}\,\%\mathrm{A}_{4\mathrm{SA}}}{100}\right) \times \mathrm{N}$$

Here, $\%A_{1SA}$, $\%A_{2SA}$, $\%A_{3SA}$ and $\%A_{4SA}$ stand for the percentages of mono-, bi-, tri- and tetra-sialylated glycans. The normalized number is multiplied by N, the number of total *N*-glycosylation sites (here, $N=3$). The value obtained for rAT was 6.73 sialic acids per protein, which was slightly higher than the value of 6.06 for nAT. This can be explained by the observed results, in which rAT had more branched structures containing tetra-sialylated tetra-antennary glycans (10.2 %).

Direct analyses of the sialic acid contents were also carried out using reverse-phase HPLC of fluorescently tagged sialic acids released by mild acid hydrolysis (Table 2). Identification of the sialic acid variants including *N*-acetylneuraminic acid (Neu5Ac) and *N*-glycolylneuraminic acid (Neu5Gc) were achieved by comparing the retention times with reference compounds (Supplementary Fig. S5). One mol of rAT was shown to have 5.42 mol of Neu5Ac and 0.07 mol of Neu5Gc. Here, Neu5Ac was the dominant sialic acid, constituting 98.7 % compared to the negligible portion of Neu5Gc (1.3 %). Their sum (5.49 mol), representing the total amount of sialic acid, was slightly lower than the 5.85 mol of Neu5Ac

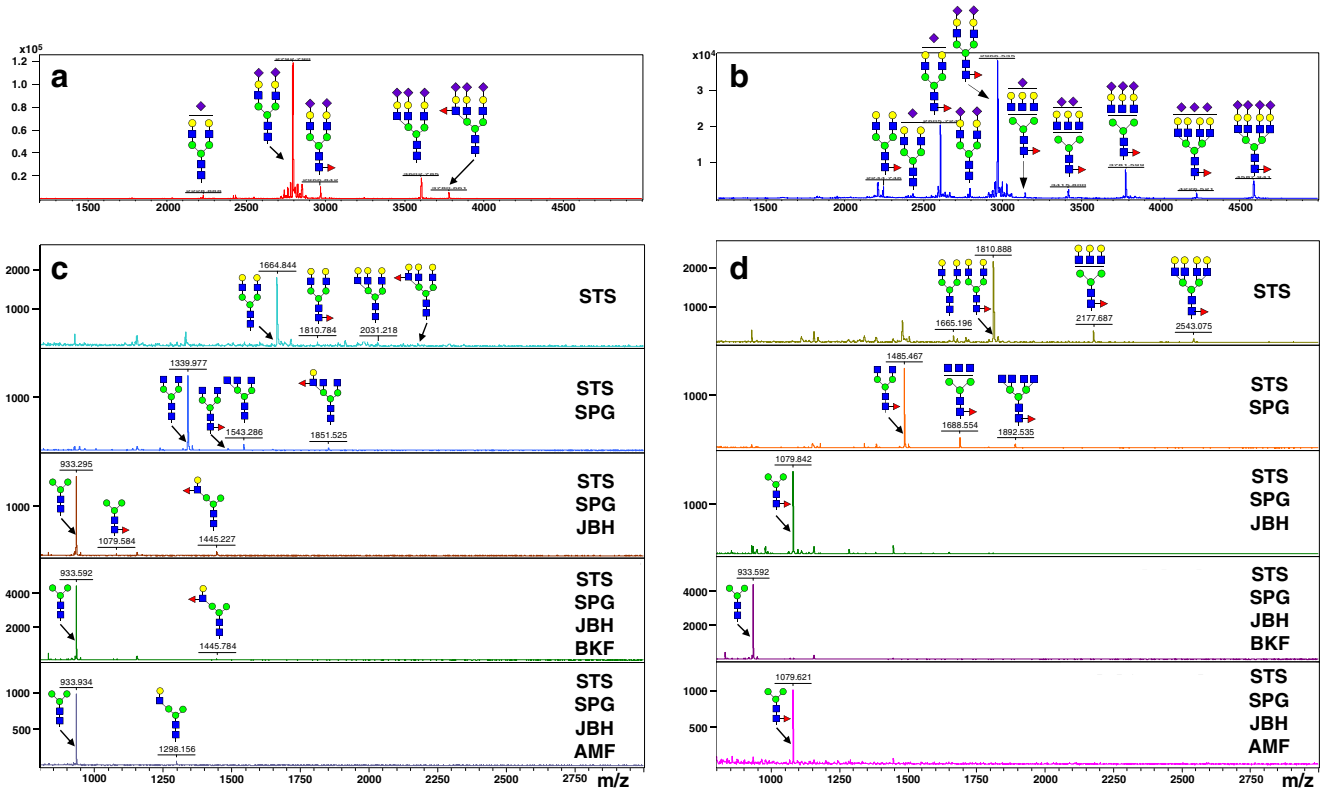

Fig. 3 MALDI-TOF mass spectra of *N*-glycans. The masses of permethylated glycans obtained from nAT (**a**) and rAT (**b**) were analyzed before exoglycosidase digestion. Also, the mass spectra of neutral glycans digested by a sialidase and a successive series of exoglycosidase digestions were obtained in the reflective positive ion mode (**c** and **d**). The abbreviations of the exoglycosidase are shown in Fig. 2 with the addition of almond meal fucosidase (AMF). Symbols for glycans are identical to those used in Fig. 2

of nAT, which is a different tendency compared to that calculated from the HPLC glycan profiles. Also, all measured amounts of sialic acid were slightly lower than the calculated values, most likely due to experimental losses which occurred during the sialic acid release and labeling steps.

Linkage analysis of sialic acids and fucoses

The linkage analysis of sialic acids was achieved by exoglycosidase digestion using *Streptococcus pneumonia* sialidase (SPS) and *Salmonella typhimurium* sialidase (STS) cleaving sialic acids with the α(2-3)-linkage and all types of linkages, respectively. Digestions of rAT glycans using both sialidases generated identical shifts of the corresponding peaks (Fig. 2b), indicating a simple α(2-3)-linkage structure as expected from the lack of β-galactoside α(2,6)-sialyltransferase activity in the CHO cells [19]. In contrast, the nAT glycans were found to contain mainly α(2-6)-linked sialic acids, as previously reported [5]. The most dominant peak (peak 3 in Fig. 2a) was bi-sialylated glycans with both α(2-6)-sialic acids. Three minor peaks were bi- (peak 2) or tri-sialylated glycans (peak 5 and 6) containing only one α(2-3)-sialic acid and the remaining α(2-6)-sialic acids.

The series of exoglycosidase digestion (sialidase, galactosidase and hexosaminidase) followed by fucosidase easily found the existence of the terminal Lewis X fucose only in the tri-antennary glycan (peak 6) of nAT (Fig. 2a), which was cross-checked by a tandem mass analysis (Supplementary Fig. S6). In the same series of digestion, the absence of exoglycosidase-resistant peak in Fig. 2b conversely indicates that all fucosylated glycans of rAT would have a core α(1-6)-fucose without a terminal fucose. This was further confirmed by digestion using a bovine kidney fucosidase (BKF) and an almond α(1-3/4)-fucosidase (AMF) (Fig. 3). All of the fucoses of rAT glycans were removed not by AMF and only by BKF, indicating the sole existence of the core α(1-6)-fucose.

The linkages of sialic acids and fucoses were also cross-checked by lectin blot assays (Fig. 4). *Maackia amurensis* (MAA) and *Sambucus nigra* (SNA) lectins, which prefer α(2-3)- and α(2-6)-linked sialic acids, selectively bind to rAT and nAT, respectively. *Aspergillus oryzae* lectin (AOL), which is known to have a preference for core α(1-6)-fucose [13, 20], specifically binds only to rAT. These patterns of lectin blots were in good agreement with the results of the linkage analysis using exoglycosidase digestion.

Table 1 *N*-glycan structures and proportions characterized by HPLC and a MALDI-TOF analysis

Peak[a]	Structure[b]	Proportion[c]	Composition[d]	Mass[e]	Deviations[f]
nAT					
1	$A2G2S^{(\alpha6)}$	6.4 %	$H_2N_2S_1(M_3GN_2)$	2431.1	−0.02
2	$A2G2S2^{(\alpha3)(\alpha6)}$	2.9 %	$H_2N_2S_2(M_3GN_2)$	2792.7	0.41
3	$A2G2S2^{(\alpha6)2}$	77.1 %	$H_2N_2S_2(M_3GN_2)$	2792.7	0.41
4	$A2G2\ F^cS2^{(\alpha6)2}$	5.2 %	$H_2N_2F_1S_2(M_3GN_2)$	2966.8	0.44
5	$A3G3S3^{(\alpha3)\ (\alpha6)2}$	3.4 %	$H_3N_3S_3(M_3GN_2)$	3602.7	0.01
6	$A3G3\ F^tS3^{(\alpha3)\ (\alpha6)2}$	5.0 %	$H_3N_3F_1S_3(M_3GN_2)$	3776.5	−0.35
rAT					
1	$A2G2F^c$	3.3 %	$H_2N_2F_1(M_3GN_2)$	2244.7	0.52
2	$A2G2S^{(\alpha3)}$	2.9 %	$H_2N_2S_1(M_3GN_2)$	2431.1	−0.10
3	$A2G2\ F^cS^{(\alpha3)}$	16.7 %	$H_2N_2F_1S_1(M_3GN_2)$	2605.7	0.42
4	$A2G2S2^{(\alpha3)2}$	2.6 %	$H_2N_2S_2(M_3GN_2)$	2792.3	0.01
5	$A2G2F^cS2^{(\alpha3)2}$	47.9 %	$H_2N_2F_1S_2(M_3GN_2)$	2966.5	0.06
6	$A3G3F^cS^{(\alpha3)}$	1.2 %	$H_3N_3F_1S_1(M_3GN_2)$	3054.5	0.01
7	$A3G3F^cS2^{(\alpha3)2}$	1.1 %	$H_3N_3F_1S_2(M_3GN_2)$	3415.8	0.10
8	$A3G3F^cS3^{(\alpha3)3}$	11.1 %	$H_3N_3F_1S_3(M_3GN_2)$	3776.7	0.16
9	$A4G4F^cS3^{(\alpha3)3}$	3.2 %	$H_4N_4F_1S_3(M_3GN_2)$	4226.5	0.42
10	$A4G4F^cS4^{(\alpha3)4}$	10.2 %	$H_4N_4F_1S_4(M_3GN_2)$	4587.9	0.47

[a] The peak numbers correspond to those designated in Fig. 2a. [b] In Ax, number (x) indicates the number of antenna (GlcNAc) on a trimannosyl core; In Gx or Sx, x represents the number of the attached galactose or sialic acid; F^c and F^t are core α(1,6)-fucose and terminal Lewis X fucose, respectively; The superscripts α6 and α3 coming after S denote the α(2-6)- and α(2-3)-linkage of sialic acids, respectively. [c] The proportion of each peak was calculated from its % area in the HPLC profile. [d] *H* hexose, *N* *N*-acetylhexosamine, *F* fucose, *S* Sialic acid, *M* mannose, *GN* GlcNAc; Here, (M_3GN_2) represents a trimannosyl core. [e] Masses were measured by a MALDI-TOF instrument. [f] Deviations indicate the differences in the measured masses from the calculated values

Inhibitory activity and *in vivo* half-life

The inhibitory activity levels of rAT and nAT were evaluated against two proteases, human neutrophil elastase (HNE) and porcine pancreatic elastase (PPE). We used chromogenic substrates to monitor the protease activity of 10 nM enzymes with and without an equimolar concentration of rAT or nAT . Both α1ATs showed very similar inhibitory activities against HNE and PPE (Fig. 5a-c). The pharmacokinetic profiles of nAT and rAT were obtained in SD rats after i.v. administration. These are shown in Fig. 5d. The measured half-life ($t_{1/2}$) of rAT was 18.5±1.2 h, which was comparable to that of nAT, 17.7±2.6.

Discussion

We expressed human α1AT, a therapeutic glycoprotein currently used for patients deficient in it, in CHO cells. Its characterization, especially focusing on the glycosylation patterns, was carefully carried out and compared to that of nAT derived from human serum. First, their equivalencies in terms of the protein level were checked by the SDS-PAGE and peptide mapping experiments. They showed the almost the same levels of electrophoretic mobility with each other in SDS-PAGE both before and after the deglycosylation process. The partial deglycosylation in the SDS-PAGE and peptide mapping experiment using the PNGase F-mediated tagging of the ^{18}O isotope confirmed that three glycosylation sites were fully occupied both in nAT and rAT. Furthermore, a comparison of the tryptic peptide mapping profiles supported the equivalency of the deglycosylated rAT and nAT.

Table 2 Sialic acid contents of nAT and rAT

Sample	Neu5Ac (mol/mol protein)	Neu5Gc (mol/mol protein)
nAT	5.85±0.27	n.d.
rAT	5.42±0.29	0.07±0.01

The sialic acid contents of nAT and rAT were carefully analyzed and compared in the present study, as it is known to be a major factor that determines the *in vivo* half-life and is therefore a typical determinant for quality control of therapeutic glycoproteins. First, the overall charge status was checked by IEF, as a negative charge of sialic acid leads to a mobility shift in the gel. The IEF pattern of rAT showed multiple isoforms similar to those of nAT, suggesting equivalency in the degree of sialylation. The average number of sialic acids attached to one protein could be obtained either through a calculation based on the HPLC glycan profile or by the direct measure of sialic acids released by

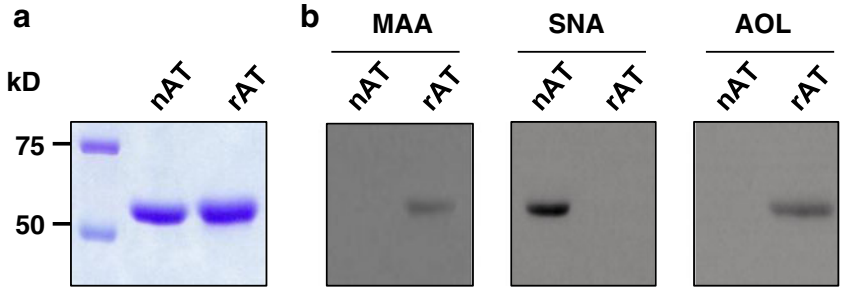

Fig. 4 Comparison of the linkages of sialic acids and fucoses by lectin blot assays. **a** The same amounts (2 μg) of nAT and rAT were subjected to 8 % SDS-PAGE and stained with Coomassie Brilliant Blue. **b** Lectin blot analyses were performed using the same amounts of samples. MAA and SNA bind to α(2-3)- and α(2-6)-linked sialic acid residues, respectively. AOL binds to fucosylated glycans with strong preference for the core α(1,6)-fucose residue

mild acid hydrolysis. Direct analysis provided somewhat lower values for both rAT and nAT compared to the values based on a calculation possibly due to experimental losses. Notably, while nonhuman sialic acid Neu5Gc was not detected in nAT, rAT was shown to contain a very low level (1.3 %) of Neu5Gc in the direct measurement. However, this amount only corresponds to 0.07 of Neu5Gc molecules attached to one rAT molecule. Interestingly, the calculated number of sialic acids (6.73) for one rAT was slightly higher than the value (6.06) for nAT, whereas the measured value

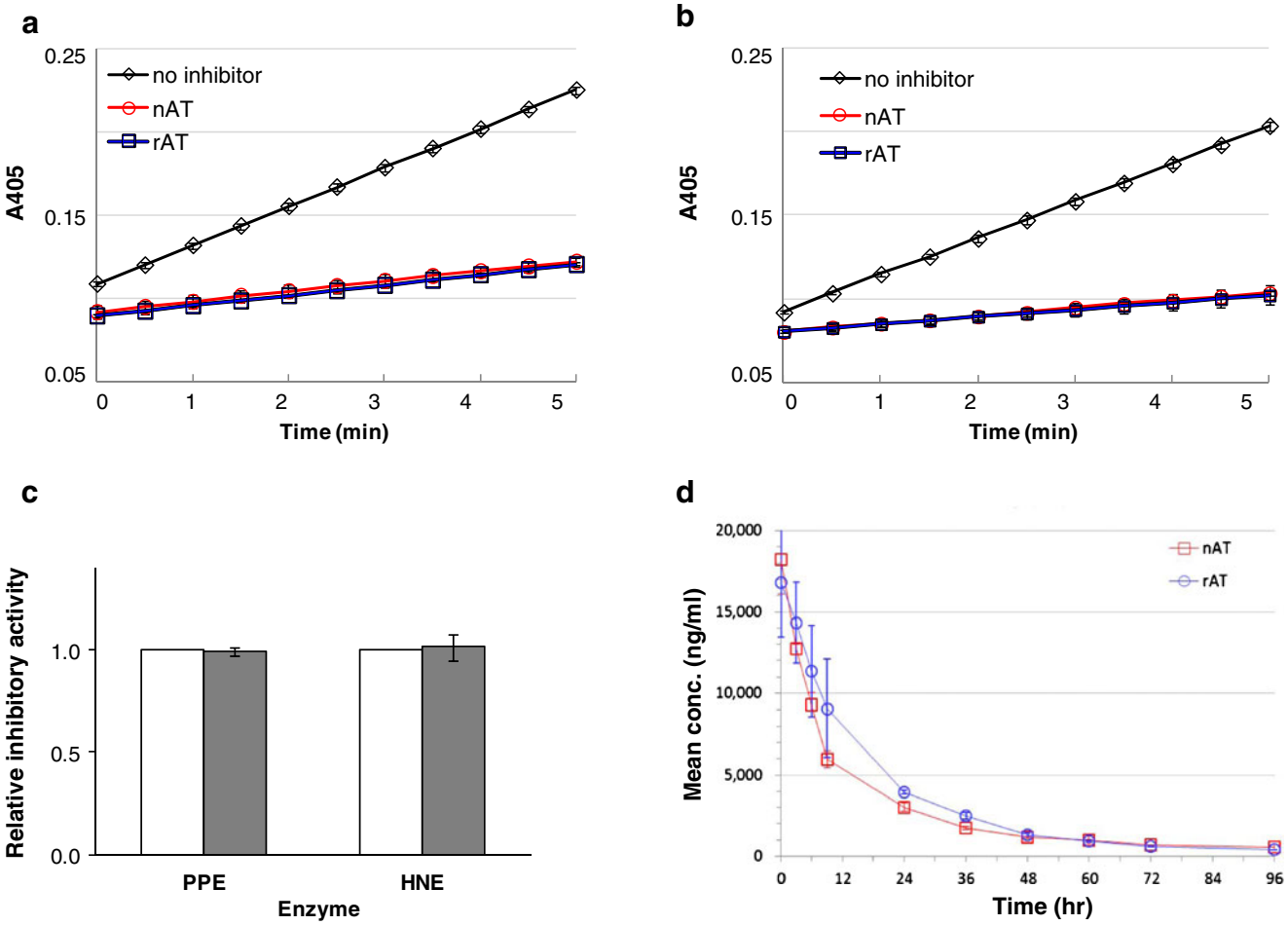

Fig. 5 Inhibitory activity and *in vivo* half-life. Enzyme activities of PPE (**a**) and HNE (**b**) were monitored in the absence (*diamond*) or the presence of nAT (*circle*) or rAT (*square*) by the absorbance at 405 nm for 5 min as described in the Materials and Methods section. Inhibitory activities of nAT and rAT were observed 74 % and 73.52 % inhibition of PPE activity and 79.27 % and 80.57 % inhibition of HNE activity, respectively. **c** The relative inhibitory activities of rAT (*filled bar*) were compared to those of nAT (*open bar*). **d** The mean concentrations (ng/ml) of nAT (*square*) and rAT (*circle*) in serum were measured following single dose i.v. administration in SD rats

(5.49) for rAT was rather low compared to the sialic acid value of 5.85 for nAT. This disagreement may originate from the bias in the calculation. However, because these tiny differences were not significant when considering experimental errors, it can be concluded that the sialic acid contents of nAT and rAT were in a comparable range.

In contrast, the glycosylation pattern of rAT was shown to be quite different from that of nAT in several aspects, including the antennary structures, fucosylation, and the linkage of sialylation. While the glycans of nAT mainly comprised simple bi-antennary structures (91.6 %) with a minor portion (8.4 %) of tri-antennary structures, rAT has more well-branched structures consisting of bi- (73.4 %), tri- (13.4 %) and tetra-antennary structures (13.4 %). The antennarity of *N*-glycan has been reported to be one of crucial factors determining the serum half-life in erythropoietin (EPO) [21, 22]. Those studies showed that EPO enriched with bi-antennary glycans (EPO-bi) had a reduced half-life in the rat as compared to usual EPO having a high content of tetra-antennary glycans. Specifically, Misaizu *et al.* suggested that the short half-life of EPO-bi resulted from the rapid clearance from systematic circulation by renal handling [21]. It was also reported that the amount of the tetrasialylated tetra-antenary *N*-glycans was the major determinant of *in vivo* half-life [23]. As far as we know, there has been no report on the relationship between the antennary structures of α1AT and its *in vivo* half-life thus far. In the present study, the half-life (18.5 h) of rAT with well-branched glycan structures containing tetrasialylated tetra-antennary glycans (10.2 %) was shown to be slightly higher than that (17.7 h) of nAT mainly containing bi-antennary glycans although the differences were within an error range. This prolonged half-life may solely result from the presence of tetrasialylated tetra-antennary glycans because the measured sialic acid content levels were comparable. Moreover, it is also noteworthy that rAT was observed to have higher amount of glycans containing exposed galactoses (asialoglycans) than nAT. The amount of asialoglycan is also important factor determining *in vivo* half-life because asialoglycoprotein receptor in the liver recognizes the exposed galactose residues without terminal sialic acid and then causes removal of the glycoproteins from circulation. Six asialoglycans (A2G2F, A2G2S, A2G2FS, A3G3FS, A3G3FS2, A4G4FS3) of rAT constitute 25.2 % of total glycan amount compared to one asialoglycan A2G2S (6.4 %) of nAT (Table 1). This higher percent of asialoglycans would induce harmful effect on the serum half-life of rAT. Therefore, it can be speculated that the positive effect caused by well-branced sialylated glycans of rAT would overcome the negative effect by higher amounts of asialoglycans and lead to the comparable or slightly higher *in vivo* half-life.

The linkage analysis results of the sialic acids and fucose of the rAT glycans represented the typical features of glycoproteins expressed in CHO cells. All sialic acids were shown to have the α(2-3)-linkage, in sharp contrast with the dominant α(2-6)-linked sialic acids of nAT. Also, most of the rAT glycans were found to have the core α(1-6)-fucose without any terminal fucose related to the antigenic epitope. On the other hand, nAT contained the terminal fucose (~8 %) of the Lewis X epitope despite the overall low level of fucosylated glycans.

We observed that rAT expressed in CHO cells had comparable levels of sialic acid content together with some portion of tetrasialylated tetra-antennary glycans, which may be beneficial for *in vivo* activity. Although several differences in the glycan profile of rAT were observed, all of them belonged to characteristic features of glycoproteins produced in CHO cells. Considering the long and wide usage history of the CHO cell expression system for therapeutic applications, the observed differences in the glycan profile are not problematic. Moreover, it was confirmed in the present study that rAT had an equivalent *in vitro* biological activity and serum half-life. Taken together, rAT produced in CHO cells would be an excellent therapeutic alternative with great advantages in manufacturing and safety issues compared to nAT derived from human plasma.

Acknowledgments We would like to thank Heung-Soo Cho and Seung-Bum Yoo for the help with the animal study. This study was supported by grants (to D.-B. Oh) from the Next-Generation BioGreen 21 Program (SSAC-PJ008001) of the Rural Development Administration and from the Korea Research Council of Fundamental Science and Technology (KRCF) and by a grant (to S. Park) from the Korea Small and Medium Business Administration (SA113037).

References

1. Wurm, F.M.: Production of recombinant protein therapeutics in cultivated mammalian cells. Nat. Biotechnol. **22**(11), 1393–1398 (2004)
2. Omasa, T., Onitsuka, M., Kim, W.D.: Cell engineering and cultivation of chinese hamster ovary (CHO) cells. Curr. Pharm. Biotechnol. **11**(3), 233–240 (2010)
3. Chung, C.H., Mirakhur, B., Chan, E., Le, Q.T., Berlin, J., Morse, M., Murphy, B.A., Satinover, S.M., Hosen, J., Mauro, D., Slebos, R.J., Zhou, Q., Gold, D., Hatley, T., Hicklin, D.J., Platts-Mills, T.A.: Cetuximab-induced anaphylaxis and IgE specific for galactose-alpha-1,3-galactose. N. Engl. J. Med. **358**(11), 1109–1117 (2008)
4. Bosques, C.J., Collins, B.E., Meador 3rd, J.W., Sarvaiya, H., Murphy, J.L., Dellorusso, G., Bulik, D.A., Hsu, I.H., Washburn, N., Sipsey, S.F., Myette, J.R., Raman, R., Shriver, Z., Sasisekharan, R., Venkataraman, G.: Chinese hamster ovary cells can produce galactose-alpha-1,3-galactose antigens on proteins. Nat. Biotechnol. **28**(11), 1153–1156 (2010)
5. Kolarich, D., Turecek, P.L., Weber, A., Mitterer, A., Graninger, M., Matthiessen, P., Nicolaes, G.A., Altmann, F., Schwarz, H.P.: Biochemical, molecular characterization, and glycoproteomic analyses of alpha(1)-proteinase inhibitor products used for replacement therapy. Transfusion **46**(11), 1959–1977 (2006)
6. Johansen, H., Sutiphong, J., Sathe, G., Jacobs, P., Cravador, A., Bollen, A., Rosenberg, M., Shatzman, A.: High-level production

of fully active human alpha 1-antitrypsin in *Escherichia coli*. Mol. Biol. Med. **4**(5), 291–305 (1987)
7. Kwon, K.S., Song, M., Yu, M.H.: Purification and characterization of alpha 1-antitrypsin secreted by recombinant yeast *Saccharomyces diastaticus*. J. Biotechnol. **42**(3), 191–195 (1995)
8. Chill, L., Trinh, L., Azadi, P., Ishihara, M., Sonon, R., Karnaukhova, E., Ophir, Y., Golding, B., Shiloach, J.: Production, purification, and characterization of human alpha1 proteinase inhibitor from *Aspergillus niger*. Biotechnol. Bioeng. **102**(3), 828–844 (2009)
9. Blanchard, V., Liu, X., Eigel, S., Kaup, M., Rieck, S., Janciauskiene, S., Sandig, V., Marx, U., Walden, P., Tauber, R., Berger, M.: *N*-glycosylation and biological activity of recombinant human alpha1-antitrypsin expressed in a novel human neuronal cell line. Biotechnol. Bioeng. **108**(9), 2118–2128 (2011)
10. Nakagawa, T., Uozumi, N., Nakano, M., Mizuno-Horikawa, Y., Okuyama, N., Taguchi, T., Gu, J., Kondo, A., Taniguchi, N., Miyoshi, E.: Fucosylation of *N*-glycans regulates the secretion of hepatic glycoproteins into bile ducts. J. Biol. Chem. **281**(40), 29797–29806 (2006)
11. Hagglund, P., Matthiesen, R., Elortza, F., Hojrup, P., Roepstorff, P., Jensen, O.N., Bunkenborg, J.: An enzymatic deglycosylation scheme enabling identification of core fucosylated *N*-glycans and *O*-glycosylation site mapping of human plasma proteins. J. Proteome Res. **6**(8), 3021–3031 (2007)
12. Packer, N.H., Lawson, M.A., Jardine, D.R., Redmond, J.W.: A general approach to desalting oligosaccharides released from glycoproteins. Glycoconj. J. **15**(8), 737–747 (1998)
13. Mun, J.Y., Lee, K.J., Kim, Y.J., Kwon, O., Kim, S.J., Lee, S.G., Park, W.S., Heo, W.D., Oh, D.B.: Development of fluorescent probes for the detection of fucosylated *N*-glycans using an *Aspergillus oryzae* lectin. Appl. Microbiol. Biotechnol. **93**(1), 251–260 (2012)
14. Goetz, J.A., Novotny, M.V., Mechref, Y.: Enzymatic/chemical release of *O*-glycans allowing MS analysis at high sensitivity. Anal. Chem. **81**(23), 9546–9552 (2009)
15. Bigge, J.C., Patel, T.P., Bruce, J.A., Goulding, P.N., Charles, S.M., Parekh, R.B.: Nonselective and efficient fluorescent labeling of glycans using 2-amino benzamide and anthranilic acid. Anal. Biochem. **230**(2), 229–238 (1995)
16. Doucet, A., Bouchard, D., Janelle, M.F., Bellemare, A., Gagne, S., Tremblay, G.M., Bourbonnais, Y.: Characterization of human prelafin mutants: full antipeptidase activity is essential to preserve lung tissue integrity in experimental emphysema. Biochem. J. **405**(3), 455–463 (2007)
17. Kolarich, D., Weber, A., Turecek, P.L., Schwarz, H.P., Altmann, F.: Comprehensive glyco-proteomic analysis of human alpha1-antitrypsin and its charge isoforms. Proteomics **6**(11), 3369–3380 (2006)
18. Llop, E., Gutierrez-Gallego, R., Segura, J., Mallorqui, J., Pascual, J.A.: Structural analysis of the glycosylation of gene-activated erythropoietin (epoetin delta, Dynepo). Anal. Biochem. **383**(2), 243–254 (2008)
19. Lee, E.U., Roth, J., Paulson, J.C.: Alteration of terminal glycosylation sequences on *N*-linked oligosaccharides of Chinese hamster ovary cells by expression of beta-galactoside alpha 2,6-sialyltransferase. J. Biol. Chem. **264**(23), 13848–13855 (1989)
20. Matsumura, K., Higashida, K., Ishida, H., Hata, Y., Yamamoto, K., Shigeta, M., Mizuno-Horikawa, Y., Wang, X., Miyoshi, E., Gu, J., Taniguchi, N.: Carbohydrate binding specificity of a fucose-specific lectin from *Aspergillus oryzae*: a novel probe for core fucose. J. Biol. Chem. **282**(21), 15700–15708 (2007)
21. Misaizu, T., Matsuki, S., Strickland, T.W., Takeuchi, M., Kobata, A., Takasaki, S.: Role of antennary structure of *N*-linked sugar chains in renal handling of recombinant human erythropoietin. Blood **86**(11), 4097–4104 (1995)
22. Takeuchi, M., Inoue, N., Strickland, T.W., Kubota, M., Wada, M., Shimizu, R., Hoshi, S., Kozutsumi, H., Takasaki, S., Kobata, A.: Relationship between sugar chain structure and biological activity of recombinant human erythropoietin produced in Chinese hamster ovary cells. Proc. Natl. Acad. Sci. U. S. A. **86**(20), 7819–7822 (1989)
23. Yuen, C.T., Storring, P.L., Tiplady, R.J., Izquierdo, M., Wait, R., Gee, C.K., Gerson, P., Lloyd, P., Cremata, J.A.: Relationships between the *N*-glycan structures and biological activities of recombinant human erythropoietins produced using different culture conditions and purification procedures. Br. J. Haematol. **121**(3), 511–526 (2003)